Reactivity of ethyl groups on a Sn/Pt(111) surface alloy

Haibo Zhao and Bruce E. Koel*

Department of Chemistry, University of Southern California, Los Angeles, CA 90089-0482, USA

Received 10 August 2004; accepted 14 October 2004

In order to probe the thermal stability and reactivity of ethyl intermediates on Pt–Sn alloy catalysts, we have synthesized these species by reaction of H atoms with adsorbed ethylene on a $(\sqrt{3} \times \sqrt{3})$R30°-Sn/Pt(111) surface alloy. Adsorbed ethyl groups are stable until 376 K where they react to evolve ethane, ethylene, and H_2. The activation energy for ethyl dehydrogenation is $E_{dehyd}* = 97$ kJ/mol, which is *twice* that reported on Pt(111). In addition, we place a lower limit of $E_{hydr}* > 70$ kJ/mol on the barrier to ethyl hydrogenation on this alloy.

KEY WORDS: ethyl; H-atom; TPD; ethylene; hydrogen; ethane; Sn/Pt alloy; dehydrogenation.

1. Introduction

Simple alkyl species have been considered for a long time to be intermediates in the conversion of saturated hydrocarbons into more economically attractive products over transition metal catalysts [1,2]. However, our knowledge of the chemistry of these species from surface science type experiments does not reflect their importance. The production of simple species such as ethyl (C_2H_5) from their fully saturated precursors is constrained heavily under UHV conditions by the significant energetic barriers to dissociative alkane adsorption. Most commonly, this problem has been surmounted by using thermal, photochemical or electron induced dissociation (EID) of ethyl halides (C_2H_5X, X = Cl, Br, I) adsorbed at low temperatures on metal single crystals [3,4]. In this manner, studies of ethyl chemistry have been reported on copper [5–9], silver [10,11], nickel [12,13], platinum [14–17], and rhodium [18]. A disadvantage of this approach is the introduction of coadsorbed halogen adatoms on the surface. Metal-ethyl compounds, like triethylbismuth [19], can also be used as thermal or photochemical precursors, but the problem of coadsorbed metal adatoms remains. Several other approaches are available that eliminate any doubts about the perturbing effects caused by coadsorbed adatoms. EID of physisorbed hydrocarbons is useful for synthesis of symmetrical alkyl and cycloalkyl species [20–26], but condensation of ethane requires a LHe-cooled probe. In heroic efforts, supersonic molecular beams [27] and hyperthermal collisions [28] have been used to cleanly create adsorbed ethyl species on Pt(111). Perhaps the most versatile approach is one pioneered by Bent and coworkers [29–31] in which incident gas-phase H atoms undergo radical addition to the π-bond in weakly adsorbed ethylene to form ethyl groups. Subsequent addition from gas-phase H atoms directly to the surface-bound alkyl is orders of magnitude slower (and any ethane formed would desorb immediately) and so the reaction is self-limiting and clean. Pt(111) is the worst substrate for using this approach, because it nearly completely rehybridizes ethylene to form a di-σ-bonded species containing essentially a C–C single bond. However, ethylene chemisorbs on most other metal surfaces retaining more double-bond character and radical addition may occur with a useful, higher probability. We decided to try this approach using Pt–Sn alloy substrates.

Bimetallic Sn/Pt supported catalysts are commercially important for suppressing the hydrogenolysis that can occur on pure-Pt catalysts [32,33]. In surface science studies, we have used well-characterized Sn/Pt(111) surface alloys as models for aspects of this catalysis involving Pt–Sn alloy phases. While we have some information on the reactivity of cycloalkyl species on these alloys [23], no information is available for ethyl groups. In related studies, we were able to use CH_3I as a precursor and thermal decomposition to form methyl (CH_3) groups on a (2×2)-Sn/Pt(111) alloy, but CH_3I was reversibly adsorbed on the $(\sqrt{3} \times \sqrt{3})$R30°-Sn/Pt(111) alloy with no decomposition during heating under UHV conditions [34]. This latter observation and the relatively high temperature for activation of the C–I bond on the (2×2)-Sn/Pt(111) alloy prompted us to turn to the use of methyl radical beams, from a pyrolytic source using azomethane, to prepare methyl groups on these surfaces. However, no such mechanism can be used to make clean beams of ethyl radicals.

Herein, we report on the synthesis of chemisorbed ethyl groups on the $(\sqrt{3} \times \sqrt{3})$R30°-Sn/Pt(111) alloy by utilizing the radical addition reaction between gas-phase H atoms and adsorbed ethylene. We investigated the

*To whom correspondence should be addressed.
E-mail: koel@usc.edu

1011-372X/05/0100–0027/0

thermal chemistry of chemisorbed ethyl groups on this Pt–Sn alloy surface without perturbation of other coadsorbed species.

2. Experimental methods

Experiments were performed in a three-level UHV chamber as described earlier [35]. The Pt(111) crystal (Atomergic; 10 mm dia., 1.5 mm thick) was prepared by 1-keV Ar^+-ion sputtering and oxygen treatments (5×10^{-7} Torr O_2, 900 K, 2 min) to give a clean spectrum using Auger electron spectroscopy (AES) and a sharp (1 × 1) pattern in low energy electron diffraction (LEED).

The $(\sqrt{3} \times \sqrt{3})$R30°-Sn/Pt(111) surface alloy was prepared by evaporating one monolayer of Sn onto the Pt(111) crystal surface and subsequently annealing the sample to 830 K for 20 s. Sn on this surface, prepared as above, is substitutionally incorporated into this surface layer at Pt-atom positions to form an alloy with $\theta_{Sn} = 0.33$, corresponding to a Pt_2Sn surface. Because of the larger size of Sn than Pt, and the importance of relieving stress in the surface layer, Sn atoms protrude 0.02 nm above the surface-Pt plane for this surface alloy [36,37]. All pure-Pt threefold sites are eliminated in the $(\sqrt{3} \times \sqrt{3})$R30° structure. For brevity throughout this paper, we will refer to the $(\sqrt{3} \times \sqrt{3})$R30°-Sn/Pt(111) surface alloy as the $\sqrt{3}$ alloy.

A Pt-tube doser was constructed, based on the design of Engel and Rieder [38] as a pyrolytic source of hydrogen atoms. The principal component is a bent Pt-tube (1 mm O.D., 0.8 mm I.D.) into which a hole of 0.1 mm diameter was mechanically drilled. The tube was resistively heated to 1275 °C, and water-cooling kept the adjacent Cu block cold. The temperature of the Pt-tube was directly measured by an optical pyrometer that was calibrated by the temperature of the Pt(111) crystal sample, as measured by a Cr/Al thermocouple. The estimated relative accuracy of the pyrometer reading was ±5 °C. The flux of H atoms obtained from this source with the Pt-tube at 800 °C and the UHV chamber pressure of 5×10^{-8} Torr was 3×10^{13} atoms cm^{-2} s^{-1}. This value was obtained by assuming that the initial sticking coefficient of H atoms on Pt(111) at 100 K was unity and using the hydrogen coverage produced from the well-known decomposition of ethylene on Pt(111) to give an absolute calibration for the H_2 yield in TPD [39]. The normal operating temperature of the Pt-tube doser during these experiments was 800 °C. This corresponds to an energy (kT) of ~0.09 eV for the incident H atoms, although it is known that similarly designed thermal atom sources do not necessarily produce atoms in a Boltzmann energy distribution [40].

H_2 (Matheson; 99.99%) was introduced via a variable leak valve (Granville-Phillips) into the Pt-tube doser after passing through a liquid-nitrogen cooled, U-tube trap. C_2H_4 (Matheson; 99.99%) was introduced via a microcapillary array doser connected to the gas line through a leak valve. All of the exposures reported here are given simply in terms of the pressure measured by the ion gauge in the UHV chamber. No attempt was made to correct for the flux enhancement of the doser or ion gauge sensitivity. Mass spectrometry performed in the UHV chamber showed no appreciable concentration of impurities in the source gases.

For all TPD experiments, the heating rate was 3.6 K/s and all exposures were given with the surface temperature at 100 K. AES measurements were made with a double-pass cylindrical mirror analyzer (CMA). The electron gun was operated at 3-keV beam energy and 1.5-μA beam current. Coverages θ_i reported in this paper are referenced to the surface atom density of Pt(111) such that $\theta_{Pt} = 1.0$ ML is defined as 1.505×10^{15} cm^{-2}.

3. Results

Ethylene chemisorbs on the $(\sqrt{3} \times \sqrt{3})$R30°-Sn/Pt(111) surface alloy as a di-σ-bonded species with a coverage of 0.27 ML in the monolayer and desorbs at 183 K in TPD [41,42]. No decomposition to produce H_2 nor hydrogenation to produce ethane occurs in TPD. In our experiments reported herein, an ethylene exposure was given to form a monolayer (saturation) coverage on the $\sqrt{3}$ alloy at 100 K, and this monolayer was then exposed to incident gas-phase H atoms for increasing amounts of time. TPD experiments were then carried out. The mass spectrometer was multiplexed to monitor many different signals simultaneously, including those at 58, 56, 54, 30, 28, 26, and 2 amu. Only ethane (30 amu), ethylene (28 amu) and H_2 (2 amu) were identified as desorption products. In particular, no C_4 products that might arise from C–C coupling reactions were detected.

Ethylene desorption spectra are shown in figure 1. The bottom curve reproduces previous reports [41,42] for ethylene adsorption and desorption in the absence, of H-atom reactions TPD spectra show that with increasing amounts of subsequent H-atom exposure, the ethylene desorption peak below 200 K, corresponding to chemisorbed ethylene, decreases in intensity while a new peak at 380 K appears and grows in size. By monitoring all of the appropriate mass signals, we conclude that this high-temperature peak is due to the combination of ethylene desorption from ethyl decomposition and a 28-amu cracking fraction arising from ethane desorption. There is also a small, reproducible peak near 250 K, but it is likely that this arises from ethyl dehydrogenation at defect sites in which Pt has a lower number of Sn neighbors (such as at an antiphase domain boundary) and are more reactive.

Figure 2 shows ethane desorption spectra in these experiments. In the absence of H-atom exposure, the

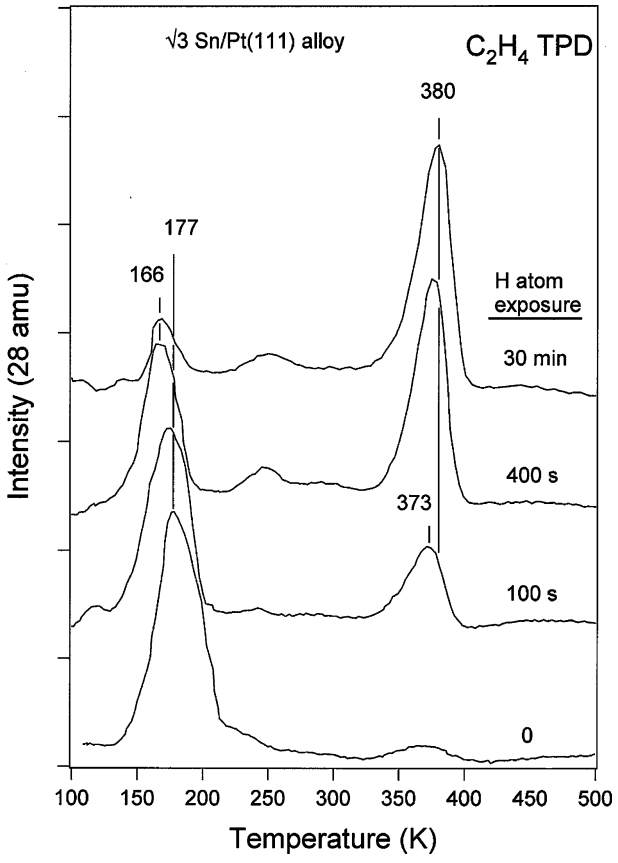

Figure 1. Ethylene (C_2H_4) TPD spectra after increasing gas-phase H-atom exposures on a chemisorbed ethylene monolayer on the ($\sqrt{3} \times \sqrt{3}$)R30°-Sn/Pt(111) surface alloy.

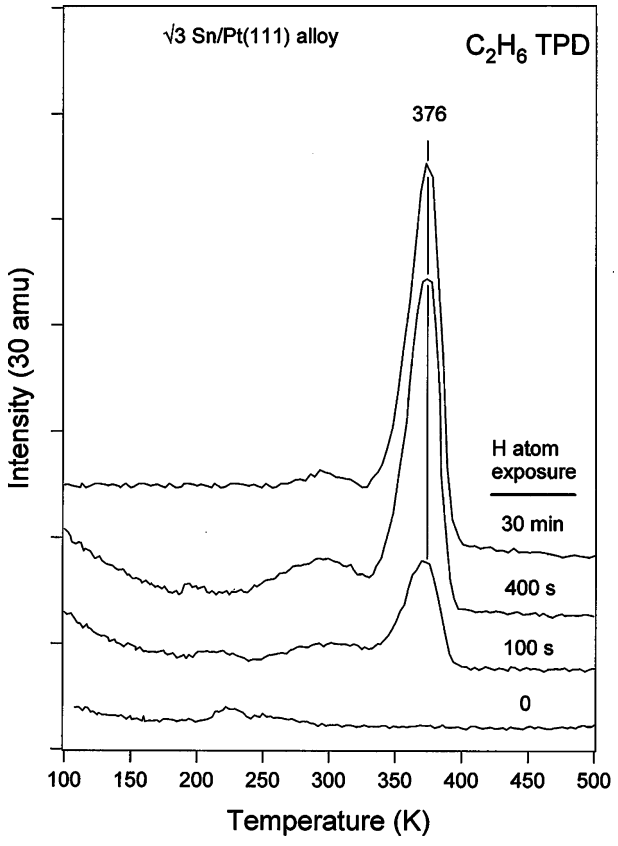

Figure 2. Ethane (C_2H_6) TPD spectra after increasing gas-phase H-atom exposures on a chemisorbed ethylene monolayer on the ($\sqrt{3} \times \sqrt{3}$)R30°-Sn/Pt(111) surface alloy.

bottom curve shows that no ethane desorption occurs after ethylene adsorption on the $\sqrt{3}$ alloy. Ethane desorption in a peak at 376 K appears and then increases in size with increasing H-atom exposures. This indicates that the amount of adsorbed ethylene that is converted to ethane increases with increasing exposures to gas-phase H atom. This is also supported by the ethylene TPD spectra in figure 1, where the ethylene desorption peak below 200 K corresponding to chemisorbed ethylene decreased in intensity with increased H-atom exposure time. A small, broad feature was observed near 300 K, but it is likely, that this arises from a small amount of ethyl hydrogenation at a few defect sites as discussed above.

Although there is no information on the desorption temperature of ethane on the $\sqrt{3}$ alloy, it must be quite low, below 100 K, and ethane adsorption must be very weak. Adsorbed *n*-butane desorbs at 153 K on the $\sqrt{3}$ alloy [43], and *n*-butane should interact about twice as strongly as ethane with the $\sqrt{3}$ alloy. This means that ethane desorption at 376 K in figure 2 must be reaction-rate limited, i.e., ethane desorbs promptly as soon as it is formed at the surface and the ethane desorption peak reveals information on the kinetics of ethane production at the surface. The only possible precursor to produce ethane at 376 K in TPD is adsorbed ethyl groups. These species are generated by the reaction between adsorbed ethylene and gas-phase H atoms.

Figure 3 shows H_2 desorption spectra in these experiments. In the absence of H-atom exposure, the bottom curve shows that little H_2 desorption occurs after ethylene adsorption on the $\sqrt{3}$ alloy. Ethylene is nearly reversibly adsorbed on this alloy. The peak below 200 K arises primarily from a cracking fraction of desorbed ethylene. With increasing H-atom exposures, an H_2 desorption peak appears at 275 K and a peak at 380 K appears and then increases in size. The H_2 desorption peak between 250 and 300 K in figure 3 is from recombination of H adatoms, and this shows that incident H atoms can still chemisorb on the $\sqrt{3}$ alloy, even though it is covered with coadsorbed ethylene and ethyl species. There are two possible origins of the H_2 peak at 380 K in addition to the cracking fraction of desorbed hydrocarbons (ethane and ethylene) that are products from ethyl dehydrogenation. Adsorbed hydrogen adatoms recombine and desorb as H_2 below 300 K on the $\sqrt{3}$ alloy [44] and so this excludes a pathway for coadsorbed H adatoms and ethyl to combine to produce ethane at 376 K. Adsorbed ethyl groups must obtain another additional H-atom from other ethyl groups to form ethane. Adsorbed ethyl species can lose one H through β-H elimination to produce ethylene and

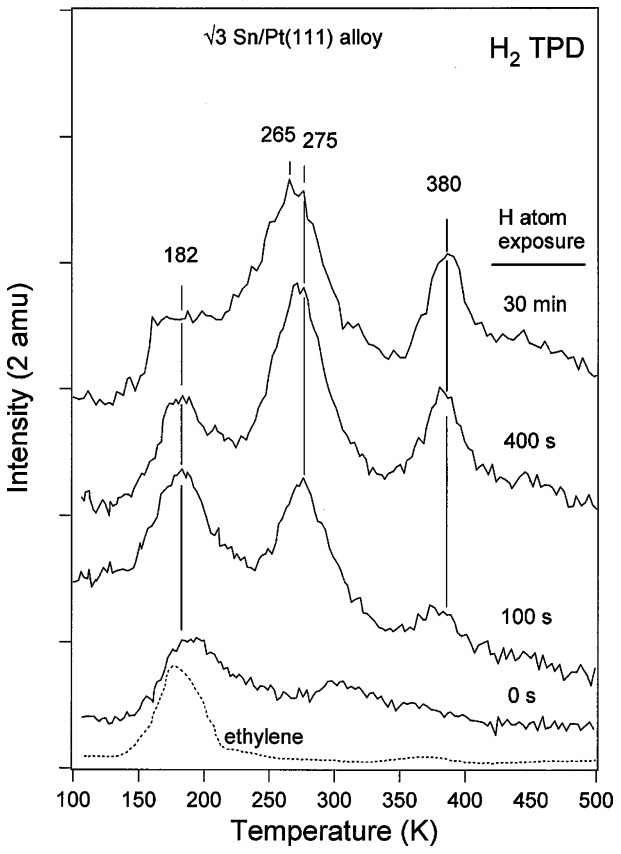

Figure 3. H_2 TPD spectra after increasing gas-phase H-atom exposures on a chemisorbed ethylene monolayer on the $(\sqrt{3} \times \sqrt{3})$R30°-Sn/Pt(111) surface alloy.

hydrogen adatoms, and this is a common pathway on most transition metal surfaces [4]. This is the most likely mechanism for the origin of the H_2 peak at 380 K. The other mechanism is for a strict disproportionation of two adjacent ethyl groups to directly yield ethane and ethylene. Ethylene does not further decompose on the $\sqrt{3}$ alloy. The peak at 380 K in figure 3 has contributions from both ethane and ethylene produced by ethyl decomposition.

No significant H_2 desorption at temperatures higher than 380 K was detected, which indicates that full decomposition of ethyl does not occur to any appreciable extent on the $\sqrt{3}$ alloy. Consistent with these H_2 TPD results, no carbon was detected by AES following TPD. Of note, no ethyl-coupling product was observed in TPD experiments by monitoring the signal at 58 amu (C_4H_{10}).

4. Discussion

There is no reaction observed between *coadsorbed* H adatoms and ethylene molecules on the $(\sqrt{3} \times \sqrt{3})$R30°-Sn/Pt(111) surface alloy [45]. The nature of gas-phase atomic hydrogen (a radical) increased the reactivity compared to surface-bound atomic hydrogen for reaction with adsorbed ethylene on the $\sqrt{3}$ alloy. Ethane formation shown in figure 2 indicates that adsorbed ethyl groups form on the $\sqrt{3}$ alloy at 100 K by radical addition of H atoms adsorbed ethylene. Adsorbed ethyl species were also created in this fashion on Cu(111) [29,30] and Cu(100) [31]. The estimated cross section for hydrogen addition to ethylene on Cu(111) was 18 Å^2 [29]. Gas-phase H- atoms have also been shown to react with di-σ-bonded cyclohexene to produce adsorbed cyclohexyl species on Ni(100) [46], even though π-bonded alkenes should have larger cross sections for radical addition reactions than di-σ-bonded alkenes. These H-radical addition reactions occur through an Eley–Rideal mechanism [4] utilizing 218 kJ/mol of potential energy per mole of H-atoms to induce reactions. Our results extend the illustrations of the utility of this process to cleanly create adsorbed alkyl species at low temperatures and thus enable studies of their subsequent chemistry.

The thermal stability and chemistry of adsorbed ethyl species on this Pt–Sn alloy is dramatically different from that on Pt(111). Adsorbed ethyl species created by dissociation of ethyl iodide (CH_3CH_2I) on Pt(111) immediately undergo a dehydrogenation step at 200 K to form chemisorbed ethylene (C_2H_4) and hydrogen adatoms via β-H elimination [15]. Although alkyl reaction to form alkenes and alkanes has been reported on Cu [6], Pt [1,3,14], and Al surfaces [47], these reactions are not commonly thought of as strict disproportionation reactions because the alkene is the dominant product. Coupling and disproportionation products were detected below 200 K upon heating adsorbed alkyl iodides on Cu(111) [7], but alkyl radicals and not surface-bound alkyl groups were proven to be the precursors to these reactions. Surface-bound alkyl groups only produce alkenes and hydrogen on Cu(111) as a result of β-H elimination.

Alloying Sn into Pt(111) greatly stabilizes adsorbed ethyl groups, and these can exist on the $\sqrt{3}$ alloy until 376 K. As discussed above, strict disproportionation reaction of adsorbed ethyl groups to produce ethane and ethylene is not observed on most metal surfaces. Disproportionation usually happens in the gas phase and in solution and this is accompanied by coupling reactions [7]. Since no coupling reactions were observed on the $\sqrt{3}$ alloy, the disproportionation reaction may not be a major reaction pathway to produce ethane and ethylene.

A reaction mechanism for dehydrogenation of adsorbed ethyl groups on the $\sqrt{3}$ alloy can be proposed as follows. As the first step, surface-bound ethyl dehydrogenates at 376 K to produce ethylene and H adatoms through β-H elimination. In the second step, some of the H adatoms generated in the first step immediately hydrogenate adsorbed ethyl groups to release ethane into the gas phase while the rest of the

H adatoms recombine to liberate H_2 from the surface as a product. The first step of β-H elimination is the rate-determining step and desorption of all products are reaction-rate limited.

Ethyl groups are more stable on the $\sqrt{3}$ alloy than any other hydrocarbon molecule reported to date, but have a stability similar to that of cyclohexyl groups on this surface [23]. The β-H elimination reaction of adsorbed cyclohexyl to produce coadsorbed cyclohexene and H adatoms was also observed on the $\sqrt{3}$ alloy at 345 K [23], but no cyclohexane was produced by hydrogenation of cyclohexyl. The reason for this apparent difference in hydrogenation reactivity between ethyl and cyclohexyl groups on the $\sqrt{3}$ alloy is not clear, but it may be due to the low cyclohexyl coverage in those experiment or the richer chemistry of cyclohexyl ligands, e.g., isomerization and/or H-shifts. The TPD spectra in figure 2 provide a good estimation for the C–H bond breaking barrier E_{dehyd}* in the dehydrogenation of surface ethyl groups. We calculate that E_{dehyd}* = 97 kJ/mol by assuming first-order kinetics and a preexponential factor of 10^{13} s^{-1}. This barrier is almost *twice* that on Pt(111) [15]. This huge increase in the C–H bond breaking barrier is due either to the general decrease in the LDOS at the Fermi energy at Pt atoms as caused by alloying Sn to Pt(111) [48] or perhaps to a loss of the specific surface electronic structure at pure-Pt threefold sites due to the loss of these sites on this alloy surface.

These results have important implications to understanding the surface science of catalysis. SFG studies of ethylene and propene hydrogenation on Pt(111) suggest that ethyl and propyl groups are reaction intermediates [49,50]. Because supported Pt–Sn catalysts are not active as catalysts in alkene hydrogenation [51,52], the poor activity of supported Pt–Sn catalysts may result from an increased barrier to form alkyl groups and/or an increased barrier to hydrogenation of these alkyl intermediates. Our studies have shown that coadsorbed H does not react with surface ethyl groups and H simply recombines and desorbs as H_2 from the $\sqrt{3}$ alloy at 275 K with an activation energy E_{d} of 70 kJ/mol. This places a lower limit on the hydrogenation activation energy barrier $E_{\mathrm{dehyd}}* = 70$ kJ/mol for surface surface-bound ethyl groups on the ($\sqrt{3} \times \sqrt{3}$)R30°-Sn/Pt(111) surface alloy.

In contrast, supported Pt–Sn catalysts are widely used in selective dehydrogenation of alkanes to alkenes [53–56]. Cortright *et al.* [57] have proposed that dehydrogenation of isobutane over $Pt/Sn/SiO_2$ catalysts is through a Horiuti–Polanyi mechanism and the first step to form adsorbed isobutyl groups is the slowest and rate-determining step. They measured a barrier of E_{dehyd}* = 85 kJ/mol to hydrogenate isobutyl with adsorbed H, and there must be a barrier of at least E_{dehyd}* = 118 kJ/mol to dehydrogenate isobutyl to form isobutene gas. Their studies also indicate that alkyl is a stable intermediate on these supported Pt–Sn catalysts. Our studies of the thermal stability of ethyl groups and the reactivity of these species with and without coadsorbed H on the $\sqrt{3}$ Sn–Pt alloy support so far the reaction mechanism and activation energies deduced for elementary steps in the reaction of alkyl species as intermediates in alkane dehydrogenation on supported Pt–Sn catalysts.

5. Conclusions

Reaction between gas-phase H atoms and adsorbed ethylene produced surface-bound ethyl groups on a ($\sqrt{3} \times \sqrt{3}$)R30°-Sn/Pt(111) surface alloy at 100 K. These ethyl groups do not dehydrogenate and are stable on the surface much above room temperature, until 376 K. C–H bond dissociation then produces ethylene and hydrogen, and this hydrogen immediately reacts to desorb as H_2 and hydrogenate coadsorbed ethyl groups to release ethane into the gas phase. The reaction-rate limited desorption of ethane can be used to provide a good estimate of the activation energy E* for breaking C–H bonds in alkyl species bound on the $\sqrt{3}$ alloy. This value of E_{dehyd}* = 97 kJ/mol is almost *twice* that on Pt(111). Ethyl groups on the $\sqrt{3}$ alloy do not react with coadsorbed H and recombination of H adatoms leads to H_2 desorption at 275 K. This observation enables us to place a lower limit on the barrier for ethyl hydrogenation on the $\sqrt{3}$ alloy of $E_{\mathrm{hydr}}* > 70$ kJ/mol. Our studies of the thermal stability of ethyl groups and the reactivity of these species with and without coadsorbed H on the $\sqrt{3}$ Sn–Pt alloy support so far the reaction mechanism and activation energies deduced for elementary steps in the reaction of alkyl species as intermediates in alkane dehydrogenation on supported Pt–Sn catalysts.

Acknowledgments

This work was supported by the Department of Energy, Office of Basic Energy Sciences, Chemical Sciences Division.

References

[1] G.C. Bond, *Heterogeneous Catalysis, 2nd ed.* (Clarendon Oxford, 1987), Ch. 8,9.
[2] G.A. Somorjai, *Introduction to Surface Chemistry and Catalysis* (Wiley, New York, 1994)Ch. 6,7.
[3] F. Zaera, Acc. Chem. Res. 25 (1992) 260.
[4] B.E. Bent, Chem. Rev. 96 (1996) 1361.
[5] J.-L. Lin and B.E. Bent, Chem. Phys. Lett. 194 (1992) 208.
[6] J.-L. Lin and B.E. Bent, J. Phys. Chem. 96 (1992) 8529.
[7] J.-L. Lin and B.E. Bent, J. Am. Chem. Soc. 115 (1993) 6943.
[8] J.-L. Lin, C.-M. Chiang, C.J. Jenks, M.X. Yang, T.H. Wentzlaff and B.E. Bent, J. Catal. 147 (1994) 250.

[9] J.-L. Lin, A.V. Teplyakov and B.E. Bent, J. Phys. Chem. 100 (1996) 10721.
[10] Z.-M. Liu, X.-L. Zhou and J.M. White, Chem. Phys. Lett. 615 (1992) 615.
[11] X.-L. Zhou, P.M. Blass, B.E. Koel and J.M. White, Surf. Sci. 271 (1992) 453.
[12] S. Tjandra and F. Zaera, Surf. Sci. 289 (1993) 255.
[13] S. Tjandra and F. Zaera, Surf. Sci. 140 (1995) 140.
[14] K.G. Lloyd, B. Roop, A. Campion and J.M. White, Surf. Sci. 214 (1989) 227.
[15] F. Zaera, Surf. Sci. 219 (1989) 453.
[16] F. Zaera, J. Phys. Chem. 94 (1990) 8350.
[17] H. Hoffmann, P.R. Griffiths and F. Zaera, Surf. Sci. 262 (1992) 141.
[18] F. Solymosi, L. Bugyi and A. Oszkó, Langmuir 12 (1996) 4145.
[19] M.E. Pansoy-Hjelvik, R. Xu, Q. Gao, K. Weller, F. Feher and J.C. Hemminger, Surf. Sci. 312 (1994) 97.
[20] X. Zhou, P.M. Blass, B.E. Koel and J.M. White, Surf. Sci. 271 (1992) 427.
[21] X. Zhou, P.M. Blass, B.E. Koel and J.M. White, Surf. Sci. 271 (1992) 452.
[22] X. Chen and B.E. Koel, Surf. Sci. 292 (1993) L803.
[23] C. Xu, Y. Tsai and B.E. Koel, J. Phys. Chem. 98 (1994) 585.
[24] D. Syomin and B.E. Koel, Surf. Sci. 492 (2001) L693.
[25] Y. Tsai and B.E. Koel, J. Phys. Chem. B 101 (1997) 4781.
[26] Y. Tsai and B.E. Koel, Langmuir 14 (1998) 1290.
[27] H.E. Newell, M.R.S. McCoustra, M.A. Chesters and C.D.L. Cruz, J. Chem. Soc., Faraday Trans. 94 (1998) 3695.
[28] D.J. Oakes, H.E. Newell, F.J.M. Rutten, M.R.S. McCoustra and M.A. Chesters, J. Vac. Sci. Technol. A14 (1996) 1439.
[29] M. Xi and B.E. Bent, J. Vac. Sci. Technol. B10 (1992) 2440.
[3] C.J. Jenks, M. Xi, M. X Yang and B.E. Bent, J. Phys. Chem. 98 (1994) 2152.
[31] M.X. Yang and B.E. Bent, J. Phys. Chem. 100 (1996) 822.
[32] Z. Karpinski and J.K. Clarke, J. Chem. Soc., Faraday Trans. I71 (1975) 893.
[33] B.H. Davis, J. Catal. 46 (1977) 378.
[34] C. Panja, E.C. Samano, N.A. Saliba and B.E. Koel, Surf. Sci. 553 (2004) 39.
[35] H. Zhao, J. Kim and B.E. Koel, Surf. Sci. 538 (2003) 147.
[36] S.H. Overbury, D.R. Mullins, M.T. Paffett and B.E. Koel, Surf. Sci. 254 (1991) 45.
[37] W.C.A.N. Ceelen, A.W. Denie vander Gon, M.A. Reijme, H.H. Brongersma, I. Spolveri, A. Atrei and U. Bardi, Surf. Sci. 406 (1998) 264.
[38] T. Engel and K.H. Rieder, in:*Structural Studies of Surfaces*, G. Höhler (ed), (Springer, Berlin, 1982) 91, p. 55.
[39] R.G. Wndham, M.E. Bartram and B.E. Koel, J. Phys. Chem. 92 (1988) 2862.
[40] C.T. Rettner, J. Chem. Phys. 101 (1994) 1529.
[41] M.T. Paffett, S.C. Gebhard, R.G. Windham and B.E. Koel, Surf. Sci. 223 (1989) 449.
[42] T. Tsai, C. Xu and B.E. Koel, Surf. Sci. 385 (1997) 37.
[43] C. Xu, B.E. Koel and M.T. Paffett, Langmuir 10 (1994) 166.
[44] M.R. Voss, H. Busse and B.E. Koel, Surf. Scl. 414 (1998) 330.
[45] H. Zhao and B.E. Koel, to be published.
[46] K.A. Son and J.L. Gland, J. Phys. Chem. B 101 (1997) 3540.
[47] B.E. Bent, R.G. Nuzzo, B.R. Zegarski and L.H. Dubois, J. Am. Chem. Soc. 113 (1991) 1137.
[48] S. Pick, Surf. Sci. 436 (1999) 220.
[49] P.S. Cremer, B.J. Mcintyre, M. Salmeron, Y.P. Shen and G.A. Somojai, Catal. Lett. 34 (1995) 11.
[50] K.R. McCrea and G.A. Somorjai, J. Mol. Catal. A:Chemical 163 (2000) 43.
[51] M. Galvagno, P. Staiti, P. Antonucci, A. Donato and R. Pietropaolo, J. Chem. Soc., Faraday Trans. 79 (1983) 2605.
[52] A. Palazov, Ch. Bonev, D. Shopov, G. Lietz, A. Sárkány and J. Völter, J. Catal. 103 (1987) 249.
[53] O.A. Barias, A. Holmen and E.A. Blekkan, Catal. Today 24 (1995) 361.
[54] R.D. Cortright, J.M. Hill and J.A. Dumesic, Catal. Today 55 (2000) 213.
[55] O.A. Barias, A. Holmen and E.A. Blekkan, J. Catal 158 (1996) 1.
[56] J.M. Hill, R.D. Cortright and J.A. Dumesic, Appl. Catal. A 168 (1998) 9.
[57] R.D. Cortright, E. Bergene, P. Levin, M. Natal-Santiago and J.A. Dumesic, Stud. Surf. Sci. Catal. 101 (1996) 1185.